

Evidence for Stimulated Scattering of Excitons into Microcavity Polaritons

F. Tassone, R. Huang, Y. Yamamoto

Erato Quantum Fluctuation Project, E. L. Ginzton Laboratory, Stanford University, Stanford, California 94305, U.S.A.

The wavefunction of a collection of identical quantum particles of integer spin (bosons) is even under exchange of the coordinates of any two of them.^{1,2} This symmetrization rule of quantum mechanics leads to stimulation of the scattering rate into final states whose population is larger than one.³ For massless photons, it is routinely observed in the laser. For massive bosons, most previous efforts concentrated in realizing the largely populated equilibrium Bose-Einstein condensate, and observing stimulated emission into it.⁴ Here we show that we do not need to produce such a condensate to observe final state stimulation. Instead, we take advantage of the highly non-equilibrium exciton reservoir and of the large polariton populations produced by external laser action on a semiconductor microcavity, and measure final state stimulation of the scattering rate of these excitons into the polaritons.

The exciton is composed of an electron and a hole (fermions), and is the equivalent of a hydrogen atom in a semiconductor. Having integer spin, it behaves as a boson, but due to its internal structure, it is not ideal. This non-ideality can be modeled as an effective interaction between fully bosonic excitons. This approximation breaks down when $n_{exc} \simeq a_B^{-d}$ (Mott density),⁵ where a_B is the exciton Bohr radius, d the dimensionality of the system. Here we are considering two-dimensional excitons confined in a GaAs 200Å quantum well embedded in a microcavity which confines the photons (inset, Fig. 1). Due to confinement, the photon is two-dimensional and acquires a finite mass. Typical dispersion relations of excitons and cavity photons are shown in Fig. 1. The exciton and photon are degenerate at the in-plane momentum $\mathbf{k}=0$. Strong dipole interaction between them results in the formation of mixed modes, the exciton-polaritons.⁶ Thus polaritons are also interacting bosons below the Mott density. The typical $k=0$ splitting between upper (UP) and lower polariton (LP) in our structure is 3.6 meV. The photon and exciton mass differ by almost 4 orders of magnitude. Already at small \mathbf{k} they become essentially uncoupled: the UP becomes photon-like, the LP exciton-like. Hereafter, we use UP and LP to refer to the strongly coupled modes at $\mathbf{k} \simeq 0$, and excitons to refer to the exciton-like LP at larger k . Due to finite transmission of the mirrors enclosing the cavity, polaritons and excitons of given k can be excited by external laser beams, with $k = \omega/c \sin \theta$, where θ is the external incidence angle, $\hbar\omega$ the photon energy, c the velocity of light. This external world coupling also results in spontaneous decay of polaritons and excitons into external photons. The polariton lifetime at $\mathbf{k}=0$ was measured $\tau_{pol} \sim 2$ ps. Excitons having $k < n\omega/c$ (n the index of refraction of the substrate) have lifetimes well over 20 ps, while those with $k > n\omega/c$ have infinite radiative lifetime as decay into external photon is forbidden by energy and momentum conservation.⁷

The thermalization process of these particles involves scattering with the lattice vibrations (phonons). As a result of the largely different masses of excitons and polaritons, the latter have a much smaller scattering rate with

phonons than the former. LP do not have time to scatter with phonons before they decay back into external photons, and do not thermalize to the lattice temperature. Instead, excitons do approximately thermalize.⁹

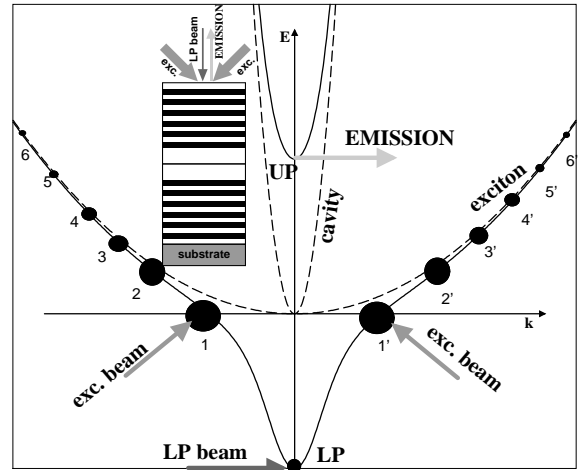


FIG. 1. Dispersion of exciton-polaritons. Exciton (not to scale) and cavity photon (dashed lines) dispersion also shown. The exciton population is depicted by solid circles of proportional size, also labelled. Typical scatterings are (c_1) $6 \rightarrow \text{UP} \pm \text{phonon}$; (c_2) $1+6' \rightarrow \text{UP}+4$; (c'_2) $1+1' \rightarrow \text{UP}+\text{LP}$. Inset: the cross section of the microcavity structure. Quarter wavelength dielectric stacks (distributed Bragg reflectors) confine the photon inside the cavity, into which a GaAs quantum well, confining the exciton, is embedded. The microcavity is grown on a substrate and mounted in a cryostat. In the experiment, two exciton beams at large angles and a LP beam at the normal direction are incident upon the top facet. The emission is also collected in the normal direction, and analyzed with a CCD spectrometer.

However, excitons are prevented to further cool down and transform into LP by a relaxation bottleneck, related to the above mentioned slow down of phonon scattering.^{10,9} Due to the short LP lifetime, the resulting LP population from this relaxation process is always small ($< 10^{-4}$ for the exciton densities considered later). Thus, injection of excitons and/or polaritons in a microcavity produces a state of the system which is far

from thermal equilibrium: the exciton and lower polariton populations can be varied *independently*. This allows to change both the initial and final state populations of the elastic scattering process where two excitons are scattered into the LP and UP respectively. In particular, the rate of emission of UP in this process is proportional to $n_{exc}^2(1 + N_{LP})(1 + N_{UP})$. Then, final state stimulation of this scattering can be induced by injection of LP using an external laser beam. The resulting $N_{UP} \ll 1$, due to the weak scattering rates and the short UP lifetime.

We realized the set-up schematically shown in the inset of Fig. 1, where two pump Ti-sapphire laser (exciton beams) of intensity I_{exc} at large angle (55°) and at the exciton energy inject an exciton population, and a third pump semiconductor laser (LP beam) of intensity I_{LP} at normal incidence and at the LP energy injects LP. These laser were continuous wave, focussed to a spot size S of about $(40\mu m)^2$. The microcavity sample was placed in a liquid He cryostat of nominal temperature $T_c = 4.8K$. Emission from the UP was collected at normal incidence and spectrally resolved from the lower polariton emission using of a CCD spectrometer. The typical emission spectrum is shown in Fig. 2, for a fixed I_{exc} and varying I_{LP} .

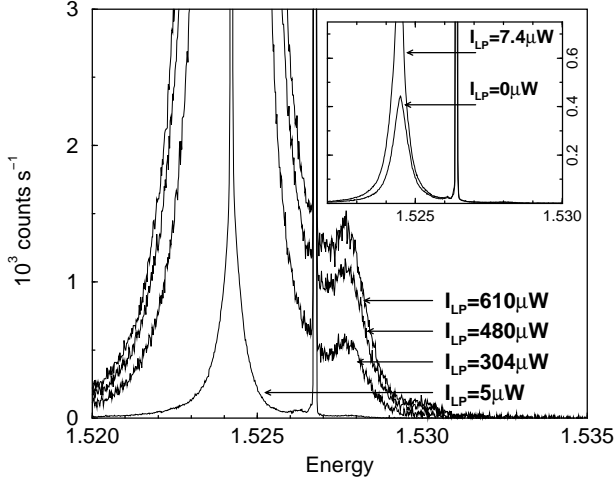


FIG. 2. Raw photoluminescence emission spectrum. Here shown for different I_{LP} , and fixed $I_{exc} = 12$ mW. Stray light diffused from the exciton beam at 55° produces a sharp peak at 1.5268 eV. Stray light diffused from the reflected semiconductor laser (LP beam) at close angles also shows at the LP energy, with the laser spectral shape, and is cut-off in the scale of the figure. In the inset, the emission for $I_{LP} = 0$, and $I_{exc} = 1$ mW. A LP population $\sim 10^{-6}$ contributed from relaxation of excitons is deduced.

The peak of emission from the UP is well resolved from the background emission of the LP. The LP spectrum is dominantly the semiconductor laser spectrum. The height of the UP emission varies with I_{LP} , and features a constant full width at half maximum close to 0.5 meV. No shifts or additional broadenings are noticed. Moreover, this holds for the available exciton beam powers

$I_{exc} < 150$ mW, and $I_{LP} < 60$ μW . It indicates absence of changes of polariton splitting or significant additional broadening by scattering with other excitons. We came to the same conclusions from reflectivity measurement at $I_{exc} = 0$ and 17mW, Fig. 3.

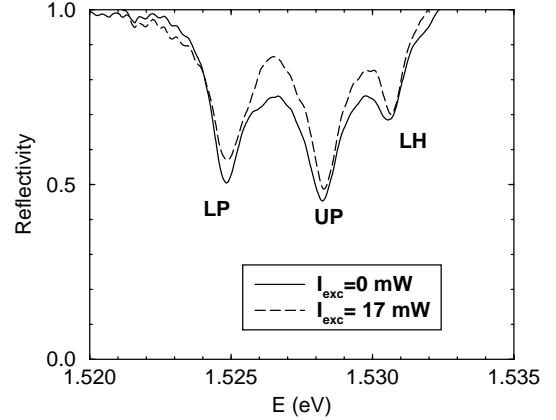


FIG. 3. The reflectivity spectra from the sample with $I_{exc} = 0$, and 17 mW. These spectra were taken using 150fs pulsed laser source centered at 1.527eV, with very weak intensity. To reduce collection time, the spectrometer resolution was lowered to around 0.5 meV. The data was then normalized with the gaussian shape of the source spectrum. Due to the very weak reflectivity signal and stronger stray light from the 17mW exciton beam, we also had to subtract spurious effects of the tails of this signal using a Lorentzian. We then fitted the reflectivity spectrum with Lorentzians. We did not find significant shifts in the position of the polariton peaks, and in their broadenings, within the spectrometer resolution. The third peak at 1.5306 eV is related to the LH exciton (4 meV above the HH exciton). The cavity is tuned in resonance with the HH exciton, so that the resulting LP and UP are mainly contributed from the HH exciton and cavity photon mode, having negligible LH components. This component smaller than 10% for both of them. Moreover, the LH exciton is irrelevant in the low temperature dynamics of the system, due to its higher energy, and consequent negligible population.

The polariton picture is thus relevant in the whole experimental range considered. Moreover, the fact that the UP emission shows its typical linewidth rules out any contribution from coherent processes like four wave mixing, in which case the emission would show a much narrower linewidth related to that of the exciton and LP lasers. This observation strongly corroborates the dynamical picture presented above, that substantial scattering of the excitons with the phonons takes place. In Fig. 4 (a) we plot typical results of the UP emission rate as a function of I_{exc} , for two different I_{LP} . In order to avoid any concerns about large exciton densities, or possible local heating of the substrate, we collected an homogeneous data set for five different I_{LP} and limiting $I_{exc} < 30$ mW. We do not include the two curves in Fig. 4 (a) in this data set, as different spot sizes and

spectrometer resolution were used to increase collection statistics. We fitted the curves in the data set with simple parabolas $dN_{UP}/dt = c_1(I_{LP})I_{exc} + c_2(I_{LP})I_{exc}^2$, for each of the five different I_{LP} . The results for c_1 and c_2 are shown in Fig. 4 (b). c_1 is independent of I_{LP} , whereas c_2 is linearly dependent on it. Since the exciton density and the LP population are proportional to I_{exc} and I_{LP} respectively, the exciton-exciton scattering into LP and UP is quadratic in I_{exc} and the stimulated part, linear in I_{LP} . Thus, Fig. 4 (b) is a direct experimental proof of final state stimulation of the exciton-exciton scattering process due to $N_{LP} > 1$.

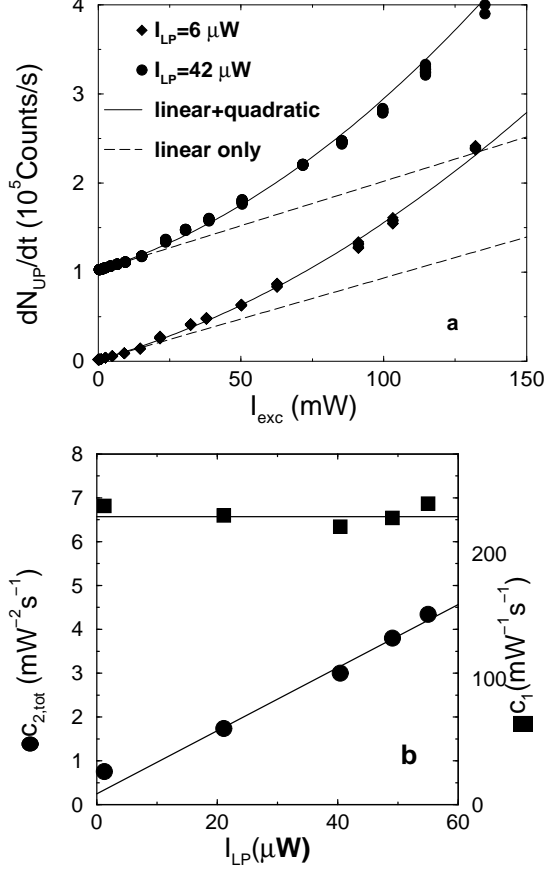


FIG. 4. Upper polariton emission rate dependence on I_{exc} and I_{LP} . a: as a function of I_{exc} , for two different I_{LP} , the highest set shifted by 10^5 for clarity. Dashed lines: the linear components only. b: the linear and total quadratic dependence on I_{exc} , as a function of I_{LP} . Solid lines: fit with a constant for c_1 and with a line for $c_{2,tot}$.

Beside the exciton-exciton scattering to LP and UP, other types of scattering take place. At finite temperature, excitons scatter with acoustic phonons to the UP.⁹ The rate of this process is linear in the exciton density, and independent of I_{LP} , thus is at the origin of the $c_1 I_{exc}$ term. Moreover, two excitons from the non-equilibrium reservoir may also elastically scatter into another exciton of lower energy and an UP. This scattering is not stimulated by LP population, but is quadratic

in exciton density. We may instead neglect UP emission from bound biexcitons produced by absorption of exciton and LP beams, as the resulting biexciton density is negligible. We calculated the scattering rates, within the Fermi golden rule, for the exciton-phonon scattering $\tilde{c}_1 = 1.1 \cdot 10^{-2} \text{cm}^2 \text{s}^{-1}$ using deformation potential interaction of excitons with acoustic phonons, for the exciton+exciton to exciton+UP $\tilde{c}_2 = 4.2 \cdot 10^{-11} \text{cm}^4 \text{s}^{-1}$, and for the exciton-exciton to LP+UP $\tilde{c}'_2 = 3.9 \cdot 10^{-13} \text{cm}^4 \text{s}^{-1}$ using the exciton-exciton exchange interaction.⁵ In order to compare theory and experiment, we need to establish how exciton density and LP populations are related to I_{exc} and I_{LP} respectively. As the exciton-phonon scattering is a well understood dynamical process, its theoretical prediction is accurate. The experimental exciton-phonon scattering rate is given by c_1/QI_{exc} , where $Q \sim 1\%$ is the measured overall detection efficiency. Apart from inaccuracies in Q , $c_1 I_{exc}$ is accurately measured, $c_1 = 230 \pm 3 \text{mW}^{-1} \text{s}^{-1}$. Thus, we have a reasonable estimate of $n_{exc} = \beta I_{exc}$ by equating the experimental and theoretical rates. We obtain $\beta = Q^{-1} c_1 / \tilde{c}_1 = 2.1 \cdot 10^6 \text{mW}^{-1} \text{cm}^{-2}$. This β is only a factor 4 smaller than the one directly estimated from the exciton lifetime $\tau_{exc} = 100 \text{ps}$,⁸ the spot surface S , and the total exciton absorption of $4 \cdot 10^{-4}$ (this small value stemming from the high top mirror reflectivity at 55° , measured 99 %). The agreement between the two independent estimates is reasonable in view of significant uncertainties in the parameters above, and in Q . We remark that $n_{exc} = 6 \cdot 10^7 \text{cm}^{-2}$ at $I_{exc} = 30 \text{mW}$, much smaller than the Mott density for GaAs QW of $2 \cdot 10^{11} \text{cm}^{-2}$.¹¹ At these n_{exc} , scattering rates are negligible in comparison with the polariton splitting and broadenings, consistently with the experimental findings above. In different experiments using similar excitation powers,¹² collapse of the polariton splitting was observed.¹³ However, there free electron-hole carriers were injected at normal incidence above the top mirror stop band (low mirror reflectivity). Hence the resulting *free carrier* density was at least 3 orders of magnitude larger than our *exciton* density, considering the longer free carrier radiative lifetime. We now estimate $N_{LP} = \gamma I_{LP} = [1 \mu\text{W}] \tau_{pol} = 8.5 \mu\text{W}^{-1}$ directly from the LP lifetime τ_{pol} , also assuming all the incident flux converted into LP. Using β , γ and Q , we would expect from theory to measure $c_2 = 1.8 \text{mW}^{-2} \text{s}^{-1}$, and $c'_2 = 0.14 \text{mW}^{-2} \mu\text{W}^{-1} \text{s}^{-1}$. Instead, we measured $c_2 = .25 \pm .17 \text{mW}^{-2} \text{s}^{-1}$, $c'_2 = .072 \pm .005 \text{mW}^{-2} \mu\text{W}^{-1} \text{s}^{-1}$. The agreement is only qualitative, yet shows we are grasping the fundamental physics of the system.

A relevant aspect of the real system is the presence of QW interface roughness and alloy disorder. It may lead to a decrease of the exciton-exciton scattering efficiency, as elastic exciton scattering on roughness perturbs the free exciton trajectories. The experimental results here indirectly show that this diffusion is instead not much relevant for the LP, as large populations in the same quantum state are required to observe stimulated scattering. This result is both due to the short cavity photon life-

time and to its small mass. As the LP is a 1:1 mixture of exciton and cavity photon, and both the cavity and LP linewidths are the same, 0.5 meV, we conclude that at least 50 % of the injected LP remain in the same quantum state, and do not diffuse to other k-states before decaying. Roughness is also at the origin of a certain surface density of strongly localized, and low energy, excitons. Due to strong confinement, they loose bosonic character, featuring a typical fermionic saturation behaviour in their population dynamics. Through this saturation dynamics, the LP beam may modulate the exciton density. However, we can exclude it, as the linear phonon scattering, proportional to n_{exc} , does not vary with I_{LP} , Fig. 4 (b), c_1 coefficient. In conclusion, our observations of stimulated emission prove that polariton beams are practical realizations of massive coherent waves, and opens the possibility of studying their peculiar bosonic properties in conventional semiconductor structures.

7090-7100 (1995)

- ¹³ Cao, H., et al., Transition from a microcavity exciton polariton to a photon laser, *Phys. Rev. A*, **55**, 4632-4635 (1997).

-
- ¹ Fierz, M., Über die relativistische Theorie kräftefreier Teilchen mit beliebigem Spin, *Helv. Phys. Acta*, **12**, 3-37, (1939).
- ² Pauli, W., The connection between spin and statistics, *Phys. Rev.*, **58**, 716-722, (1940).
- ³ Einstein, A., Zur Quantentheorie der Strahlung, *Physikalische Zeit.*, **18**, 121-128 (1917).
- ⁴ Mysyrowicz, A., Benson, E. & Fortin, E., Directed beam of excitons produced by stimulated scattering, *Phys. Rev. Lett.* **77**, 896-899, (1996).
- ⁵ Hanamura, E. & Haug, H., Condensation effects of excitons, *Phys. Reports* **33**, 209-284, (1977).
- ⁶ Weisbuch, C., Nishioka, M., Ishikawa, A. & Arakawa, Y., Observation of the coupled exciton-photon mode splitting in a semiconductor quantum microcavity *Phys. Rev. Lett.* **69**, 3314-3317, (1992).
- ⁷ Agranovich, V. M. & Dubovskii, O. A., Effect of retarded Interaction on the Exciton Spectrum in one-dimensional and two-dimensional Crystals, *JETP Lett.*, **3**, 223-226, (1966).
- ⁸ Andreani, L.C., Tassone, F. & Bassani, F., Radiative lifetime of free excitons in quantum wells, *Solid State Comm.*, **77**, 641-645, (1991).
- ⁹ Tassone, F., Piermarocchi, C., Savona, V., Quattropani, A. & Schwendimann, P., Bottleneck effects in the relaxation and photoluminescence of microcavity polaritons, *Phys. Rev. B* **56**, 7554-7563, (1997).
- ¹⁰ Toyozawa, Y., On the dynamical behavior of an exciton, *Suppl. Progr. Th. Physics*, **12**, 111-140, (1957).
- ¹¹ S. Schmitt-Rink, s, Chemla, D.S. & Miller, D.A.B., Linear and nonlinear optical properties of semiconductor quantum wells, *Advances in Physics*, **38**, 89-188, (1989).
- ¹² Pau, S., Bjork, G., Jacobson, J., Cao, H. & Yamamoto, Y. Stimulated emission of a microcavity dressed exciton and suppression of phonon scattering, *Phys. Rev. B*, **51**,